



Potential Fuel Economy Improvements from the Implementation of cEGR and CDA on an Atkinson Cycle Engine

2017-01-1016
Published 03/28/2017

Charles Schenk and Paul Dekraker

US Environmental Protection Agency

CITATION: Schenk, C. and Dekraker, P., "Potential Fuel Economy Improvements from the Implementation of cEGR and CDA on an Atkinson Cycle Engine," SAE Technical Paper 2017-01-1016, 2017, doi:10.4271/2017-01-1016.

Abstract

EPA has been benchmarking engines and transmissions to generate inputs for use in its technology assessments supporting the Midterm Evaluation of EPA's 2017-2025 Light-Duty Vehicle greenhouse gas emissions assessments. As part of an Atkinson cycle engine technology assessment of applications in light-duty vehicles, cooled external exhaust gas recirculation (cEGR) and cylinder deactivation (CDA) were evaluated. The base engine was a production gasoline 2.0L four-cylinder engine with 75 degrees of intake cam phase authority and a 14:1 geometric compression ratio. An open ECU and cEGR hardware were installed on the engine so that the CO₂ reduction effectiveness could be evaluated. Additionally, two cylinders were deactivated to determine what CO₂ benefits could be achieved. Once a steady state calibration was complete, two-cycle (FTP and HwFET) CO₂ reduction estimates were made using fuel weighted operating modes and a full vehicle model (ALPHA) cycle simulation. This paper presents the results from implementation of cEGR and CDA on an engine capable of Atkinson cycle operation.

Introduction

In 2012, EPA promulgated a final rulemaking to set light-duty vehicle greenhouse gas (GHG) emissions standards for vehicles sold in model years 2017-2025 [1]. This action was part of a joint rulemaking with the National Highway Traffic Safety Agency (NHTSA) in which NHTSA established CAFE standards for the same model years. This rulemaking included a commitment by the EPA to perform a Mid-Term Evaluation (MTE) to review industry progress toward the 2022-2025 GHG standards. This paper presents results from part of the EPA progress review that was finalized in 2017 [18]. EPA conducted a series of engine benchmarking and development activities at its National Vehicle Fuel and Emissions Laboratory in Ann Arbor, MI.

Two of the future technologies assessed in the 2012 rulemaking were cEGR and CDA. In earlier work published by EPA, 1-D gas dynamics and 0-D combustion modeling was conducted using a Gamma Technologies GT-POWER™ model of an Atkinson cycle

engine with these technologies [2]. In this investigation, a base Atkinson engine map was obtained from dynamometer testing of a U.S. certified 2.0L 13:1 CR Mazda SkyActiv engine. GT-POWER™ was used to simulate the effect on BSFC of increasing compression ratio and adding cEGR and CDA.

This paper continues the investigation into potential GHG improvements when adding cEGR and CDA to an Atkinson engine with a 14:1 geometric compression ratio. Hardware was acquired to further understand the effectiveness of both cEGR and CDA from engine testing and to validate the technology performance estimates previously generated using GT-POWER™. The potential two-cycle CO₂ improvements were estimated from both steady state data and the vehicle simulation model ALPHA for a future vehicle.

The term GHG encompasses CO₂, methane, air conditioning refrigerants, and other gases that contribute to global warming. In this paper, GHG improvements were taken to be CO₂ reductions characterized by brake thermal efficiency (BTE) improvements and cycle CO₂ reductions using the same fuel in the base and test cases. Normally BSFC (fuel flow (g/hr)/power (kW)) would be used to evaluate engine performance. But BSFC does not take into account the energy or carbon content of the fuel which can vary substantially between fuels (e.g. with ethanol content). BTE (Equation 1) was used to normalize gasoline energy content (net heating value). Fuel flow is directly proportional to CO₂ for a given fuel. Since fuel flow is in the denominator, for a given power output a higher BTE correlates to lower CO₂ emission. The testing in this paper only used one fuel so that BTE improvement percentages were equivalent to CO₂ emission reduction percentages without need for fuel carbon content correction.

$$BTE (\%) = \frac{\text{brake power (kW)}}{\text{fuel flow (g/s)} * \text{net heating value (kJ/g)}} * 100 \quad (1)$$

Background

The effectiveness of cEGR has been studied as a means to mitigate combustion knock and improve fuel efficiency, particularly in boosted engines [3,4,5]. At high load, cEGR can reduce or eliminate the need for enrichment that would otherwise be needed for knock and temperature control. By reducing the tendency to knock, cEGR can be used to maintain best BTE combustion phasing for improved efficiency. cEGR can also benefit efficiency at part-load conditions by reducing pumping work. Though cEGR displaces fresh air in the cylinder, boost can be increased to maintain the desired power. This is not the case for naturally aspirated engines where cEGR added at high loads will result in a loss of power.

Cylinder deactivation [6, 7, 8] is a known method for reducing part-load CO₂ emissions that is already in use today. CDA is expected to see even wider application to meet future GHG standards. Deactivating one or more cylinders at light- to mid-loads (i.e., under approximately 50% of peak BMEP) can reduce pumping losses by increasing the load, throttle angle, and intake manifold pressure of the operating cylinders. NVH issues are one of the limiting factors for this approach. NVH can limit the speed and load where CDA is possible as well as add cost due to additional hardware required for NVH mitigation. Other factors such as oil control can also limit the effectiveness of this approach by requiring periodic reactivation of cylinders.

CDA and cEGR could further improve the efficiency of an Atkinson cycle engine. Atkinson engines derive their efficiency from late intake valve closing that effectively limits compression while maintaining a higher expansion ratio [9, 10, 11]. The higher expansion ratio improves efficiency as does the reduction in pumping work due to the intake cam phasing controlling airflow rather than using a throttle valve for control. The advent and widespread use of electronically controlled throttles and fast, wide range intake cam phasers has made it possible for production engines with very high compression ratios (13:1 or more) to use Atkinson cycle over part of the operating range and still maintain adequate BMEP [12, 13, 14].

Future Atkinson Cycle Engine Evaluation

Engine Description

A production engine was obtained to conduct cEGR and CDA validation work. This engine was a naturally aspirated direct-injection 2014 Mazda 2.0L from a European Mazda6. Table 1 summarizes the engine specifications. The engine was similar to a previously benchmarked engine [16] except it was optimized for the higher octane gasoline available in Europe. It utilized a 14:1 geometric compression ratio, which was an increase from the 13:1 of the North American versions of this engine. Tier 2 certification gasoline was used in this testing (Table 2).

Table 1. 2014 Mazda 2.0L specifications

Displaced volume	1998 cc
Stroke	91.2 mm
Bore	83.5 mm
Compression ratio	14:1
Rated power	115 kW @ 6000 RPM
Rated torque	203 Nm @ 4000 RPM

Table 2. Measured test fuel properties

Tier 2 Certification Gasoline	
RON	96.6
MON	88.9
Distillation Properties (°C) D86	IBP
	10%
	50%
	90%
	FBP
Ethanol content (% vol) D5599	0.0
Sulfur content (ppm) D2622	39.6
Aromatics (% vol) D1319	31
Vapor pressure (kPa) D5191	62
Net Heating Value (MJ/kg) D240	42.82
API gravity (degrees) D4052	58.9
Density (g/cm ³) D4052	0.7424

Test Setup

The engine was benchmarked at EPA's National Vehicle and Fuel Emissions Laboratory in an engine dynamometer test cell. A photograph of the test setup is shown in Figure 1. Additional details of this test setup, including instrumentation, were consistent with previous EPA benchmarking programs [16]. The engine was instrumented to measure temperatures and pressures of the intake manifold, exhaust manifold, and engine oil. Each cylinder had cylinder pressure and spark command logged on a high speed data acquisition system. Gaseous emissions were measured with a Horiba MEXA 7100DEGR which included intake manifold CO₂ measurement for calculation of cEGR rate (Equation 2). A Micro Motion fuel flow meter was the primary fuel measurement which was confirmed by gaseous-emissions carbon balance.

$$cEGR (\%) = \frac{(Intake\ CO_2\ (ppm) - Ambient\ CO_2\ (ppm))}{Exhaust\ CO_2\ (ppm) - Ambient\ CO_2\ (ppm)} * 100 \quad (2)$$

The unmodified 14:1 engine was first benchmarked using a factory ECU. In addition to providing baseline CO₂ emissions, the benchmark data was used to establish tables for the spark timing, fuel injection events, and phase angle for both cams. This provided a starting point for calibrating cEGR.

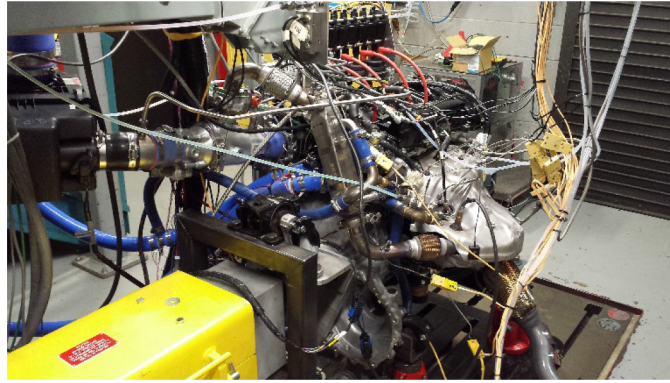


Figure 1. Test setup with cEGR system installed

Engine performance maps were created using an automated test cell routine. This routine controlled the engine to specified speed and torque values and then waited for torque, fuel, and exhaust temperature stability criteria to be met. When the engine was stable, the engine conditions, emissions, and fuel rate data were then logged.

Results

Calibration Development

A map of the OEM engine calibration and performance was taken first as a reference for the cEGR and CDA results. Figure 2 shows that this engine was over 35% BTE from about 1750 rpm to almost 4000 rpm between 120 Nm and 150 Nm. The peak BTE was 36.7%.

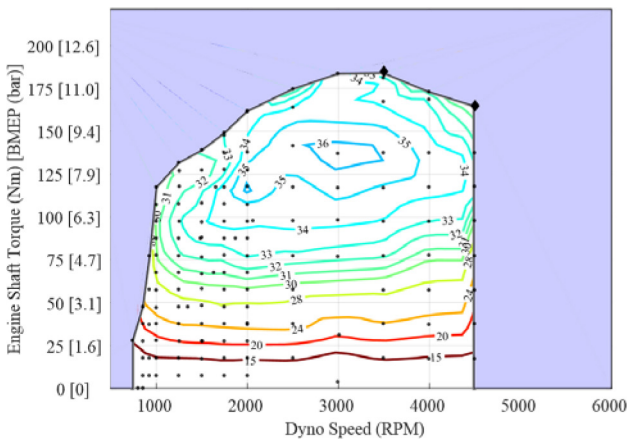


Figure 2. Baseline 14:1 BTE with OEM engine hardware and ECU

A cEGR system was designed and built by Southwest Research Institute (SwRI). This system (Figure 3) consisted of an exhaust pickup upstream of the exhaust catalyst (TWC), an EGR cooler, a butterfly-style EGR valve, and a mixer with a second intake throttle (inlet mixer) valve upstream to generate additional EGR driving pressure. The venturi mixer was adopted from a natural gas application and incorporated a venturi with radial EGR introduction to improve mixing. A universal exhaust gas oxygen (UEGO) sensor was installed downstream of the mixer to measure intake O_2 concentration. The cEGR control used PID controls on the actuators to achieve the desired intake O_2 concentration. Intake manifold CO_2 and exhaust CO_2 measured by Horiba MEXAs were used to calculate the cEGR rates (Equation 2).

A Continental SCP-2 electric water pump circulated engine coolant to maintain a maximum 5 °C coolant temperature rise across the EGR cooler. The pump consumed a maximum of 0.26 kW at the maximum cEGR mass flow point which had a 50 kW brake output or 0.5% of engine brake power. Power consumption was typically near 0.1 kW. The power consumed by the coolant pump was included in the BTE calculations.

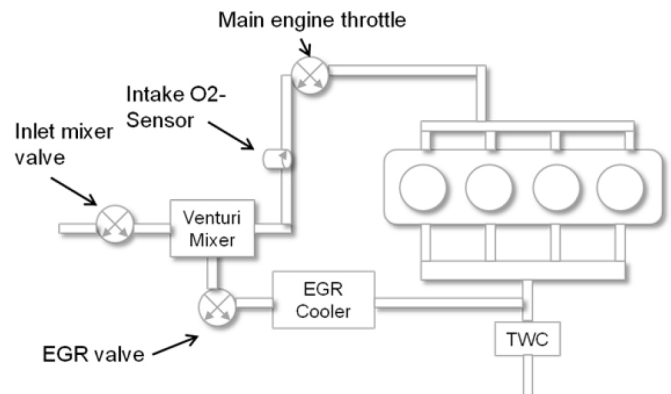


Figure 3. cEGR system functional schematic diagram

Since early cEGR tests showed that the OEM ignition system was not able to consistently maintain COV of IMEP below 5%, a dual coil offset ignition system (DCO[®]) was sourced from SwRI [17]. This system switches between two coils per cylinder to increase spark duration. The duration of the spark could be controlled up to 12 coil switches which was about 60 CAD at 2000 rpm. The spark energy was also higher, 274 mJ/spark for the OEM ignition system vs 480 mJ/ 1st switch + 200 mJ/additional switch for the DCO system. Only one coil switch was necessary for most operating conditions, and no more than 3 switches (880 mJ/spark) were required to achieve <3% COV. The additional ignition power was subtracted from engine power for calculating BTE.

An M670 OpenECU[®] from Pi Innovo was used in place of the OEM engine control unit (ECU). The OpenECU[®] allowed full control of all engine hardware and algorithms. Simulink[®] EGR control algorithms were sourced from SwRI and integrated into the OpenECU[®] code to speed development.

To focus calibration development where it would have the most significant CO_2 reduction impacts, the engine operating range over the FTP and HwFET GHG regulatory cycles was used as a guide. A previous paper [16] investigated potential two-cycle GHG emissions

for a future vehicle with the 13:1 2.0L version of this engine. This vehicle was a 2008 Mazda6 with 10% weight reduction, 20% rolling resistance and aerodynamic drag reductions along with a future 8 speed transmission. Part of the future powertrain management strategy was to down-speed the engine for lower CO₂ emissions. HIL testing of this vehicle showed that more than 90% of the two-cycle engine speeds were below 1750 rpm (Figure 4). Referencing these speeds and loads, the cEGR optimization was focused below 2000 rpm and 137 Nm.

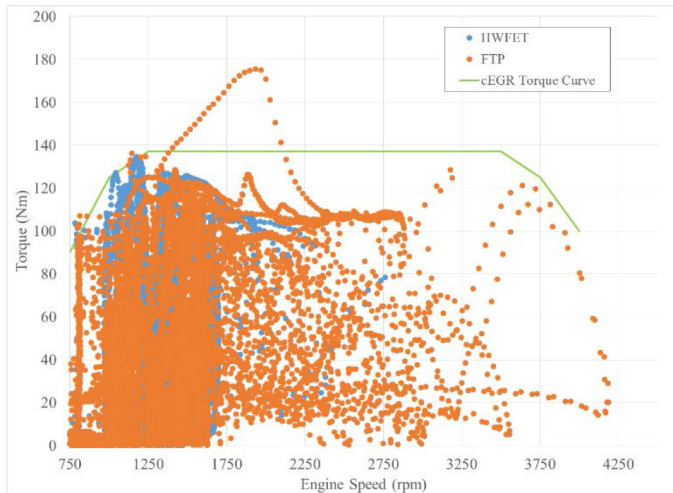


Figure 4. Two-cycle operating points for a 2014 Mazda3 with automatic transmission

Calibration was performed by stepping through the ECU control tables and adding cEGR, then adjusting spark and intake cam phase. cEGR was added until either the COV increased to 3% or BTE started to decrease at constant speed and load. Spark was adjusted to maintain the 50% burn location (CA50) around 8° ATDC or observed best BTE location. At higher loads (>100 Nm) CA50 timing was typically knock limited and set 2 degrees retarded from the onset of knock. The intake cam phase had to be advanced with increasing cEGR at mid-loads where the intake charge is controlled by the intake valve phasing using the Atkinson cycle. The advance was necessary to increase the trapped intake charge by the amount of cEGR added to the fresh air flow. At operating conditions where the intake cam was not controlling intake charge, the engine throttle was opened to increase the intake charge. This calibration method was used from idle to 4000 rpm and up to 137 Nm with the focus on best performance below 2000 rpm.

cEGR Maps

The resulting cEGR map (Figure 5) shows peak rates of 22% around 2000 rpm, 100 Nm. Above 100 Nm cEGR had to be progressively replaced with fresh air in order to achieve the desired loads. Below 1250 rpm internal EGR (iEGR) was found to give higher BTE than cEGR. The exhaust cam phase was used to control iEGR through overlap with the intake valve event. Spark was advanced to achieve best BTE. iEGR rate was not measured. Figure 5 shows the range where iEGR was used with little or no cEGR.

Best BTE CA50 phasing (Figure 6) was possible up to 100 Nm, but above that CA50 had to be retarded to avoid knock. The resulting BTE map (Figure 7) peaked at 37.6% with a 36% island that extends from 80 Nm to 120 Nm between 1000 and 2500 rpm. Figure 8 shows

the BTE improvement (Equation 3) tapers off at high loads where there is no additional flow capacity for cEGR. The peak cEGR BTE range more closely aligns with engine two-cycle speed (1000-1750 rpm) and load (0-120 Nm) ranges over the regulatory cycles than the non-cEGR baseline case, which peaks well above 2000 rpm (Figure 2). Above 137 Nm or 4000 rpm no cEGR was used so the calibration was the same as the production engine.

$$BTE \text{ improvement } (\%) = \frac{(BTE_{cEGR} - BTE_{base})}{BTE_{base}} * 100 \quad (3)$$

Where BTE_{cEGR} was the BTE (%) with cEGR and BTE_{base} was BTE (%) of the base engine without cEGR as described in Figure 2.

cEGR heat rejection rate was calculated from thermocouple measurements of the temperature drop across the EGR cooler and cEGR rate. Heat rejection peaked at 3.7 kW (Figure 9) which was an approximately 10% increase in coolant heat rejection rate at this operating condition. cEGR was reduced to zero at higher loads and engine speeds so that the maximum coolant heat rejection rate would not change. cEGR in this case would not necessarily require a larger radiator, though it would potentially impact the use of grill shutters, radiator fan duty cycle, and other thermal management systems. These vehicle system impacts were not considered in this paper.

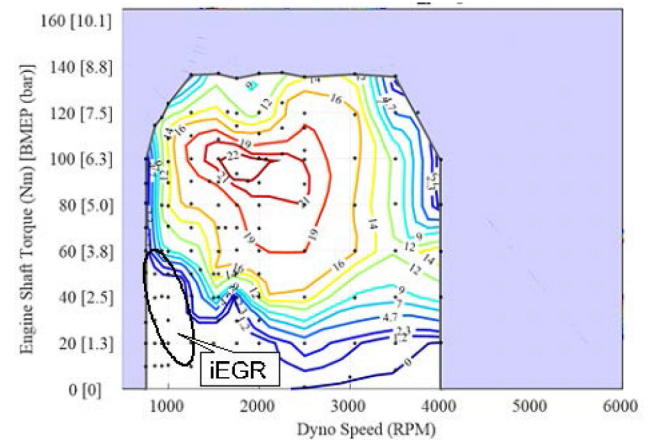


Figure 5. cEGR (%)

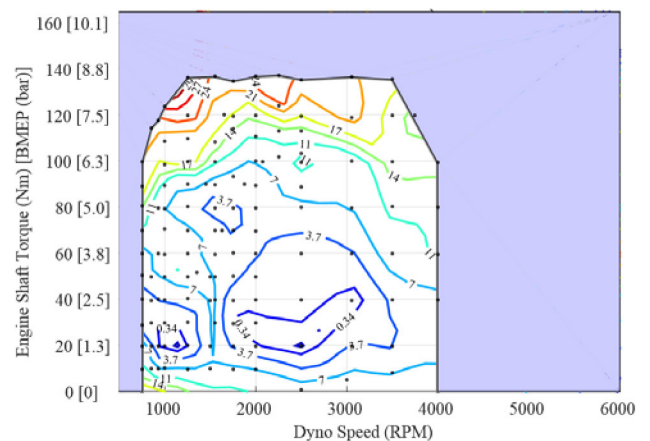


Figure 6. CA50 (°ATDC) with cEGR

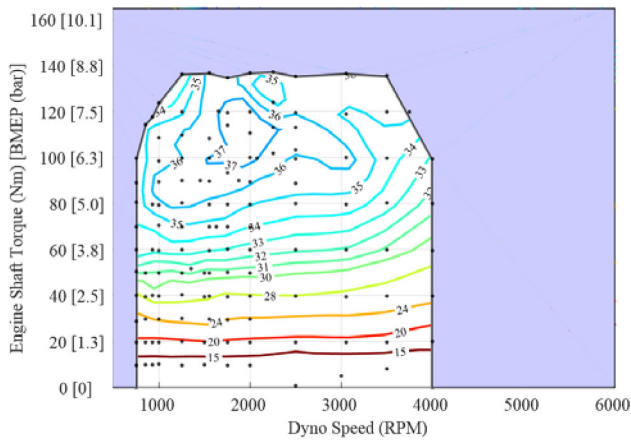


Figure 7. BTE (%) with cEGR

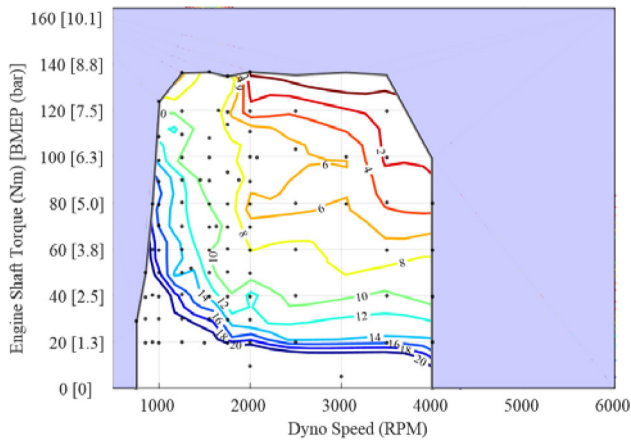


Figure 8. BTE Improvement (%) over no-cEGR baseline

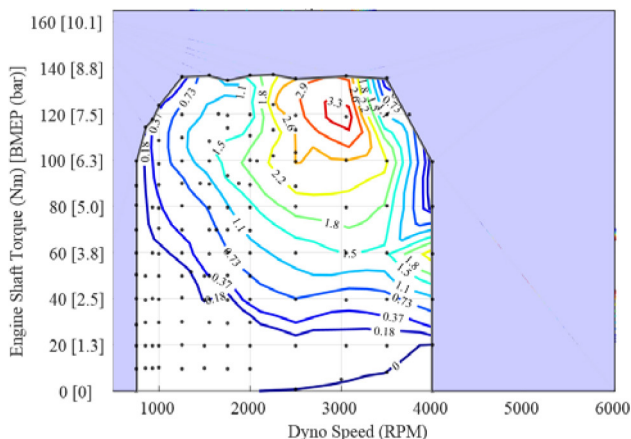


Figure 9. Heat rejection (kW) from EGR cooler

Figure 10 shows the 10% to 90% combustion duration with cEGR. Previous studies [14, 15] have shown that the best combustion duration for efficiency and knock mitigation was about 20 CAD. The combustion durations for this engine with cEGR were considerably longer. In some regions they were almost three times the desired duration. This indicates that cEGR could be more effective with a properly integrated and optimized engine design. Higher in-cylinder motion through redesigned intake ports, the use of tumble-inducing variable-geometry intake manifold, and revised combustion chamber geometry could be used to reduce burn duration.

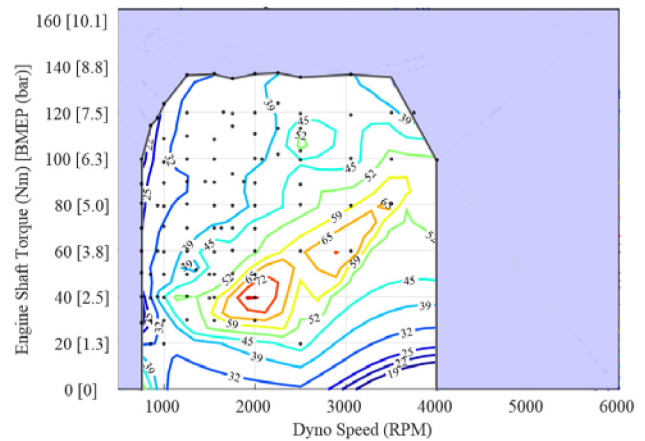


Figure 10. 10-90% combustion duration (CAD) with cEGR

CDA and cEGR Maps

To simulate CDA the rocker followers for cylinders two and three were removed to permanently deactivate the valves in those cylinders. The hydraulic lifters were also removed and replaced with o-ringed plugs. This configuration is not strictly realistic for a number of reasons (NVH, oil control, trapped air, etc.) but should give an approximate indication of what benefits might be possible with CDA in this application. Fuel and spark were turned off in the two deactivated cylinders. For simplicity of demonstration the ECU software was configured so that the two running cylinders would operate using the four-cylinder calibration for spark, cam phasing, fuel injection, and EGR rates. For example, at a measured CDA point of 40 Nm, the two firing cylinders would be operating with the 80 Nm four-cylinder calibrations at the same IMEP. No attempt was made to optimize the CDA calibration.

Once the ECU code was prepared for CDA, a speed range was determined by running with the cylinders deactivated from 1000 to 2500 rpm. No changes were made to the driveshaft or engine hardware beyond removal of the rockers and lifters. By visually assessing engine vibration it was determined that operation below 1300 rpm would not be advisable without NVH measures. The focus of this test was strictly to investigate the possible part load CO₂ reduction. NVH mitigation and optimized CDA controls may result in different CO₂ emissions benefits than those obtained in this test.

Data were collected in the area shown in Figure 11. The contour lines are the percentage BTE improvement (Equation 3) from four-cylinder cEGR operation. The improvement from CDA ranged from over 25% below 20 Nm to a disbenefit above about 50 Nm. The losses from the deactivated cylinders caused the disbenefit to occur at lower loads than might be predicted by where the two firing cylinders would be running on the four-cylinder BTE map. On the four-cylinder map (Figure 7), 2000 rpm, 50 Nm CDA would be about 100 Nm which is in the peak BTE island of 37%. With CDA the BTE (Figure 12) peaked at 33%. The losses associated with the deactivated cylinders caused a 3-7% (absolute) drop in BTE during CDA operation. A rough estimate of the deactivated cylinder losses was calculated from the ECU load and the actual load (Figure 13).

Since the trapped air in the deactivated cylinders was not replenished, these losses were higher than might be achieved with switchable deactivation hardware. By not replenishing the trapped air this

demonstration did not have the full benefit of the air spring effect to reduce lost work [6]. The same inability to switch CDA on and off during engine operation also omitted the disbenefit caused by the need for oil control and to maintain thermal uniformity (the deactivated cylinders cause uneven head/block/piston temperatures) that would require periodically turning off CDA. The losses from the less than optimum air spring were continuous and probably outweigh the impact of periodically turning off CDA for oil control and engine thermal uniformity. The net result was that the observed CDA improvements, minus NVH considerations, should be a conservative CO₂ reduction estimate of a working CDA system.

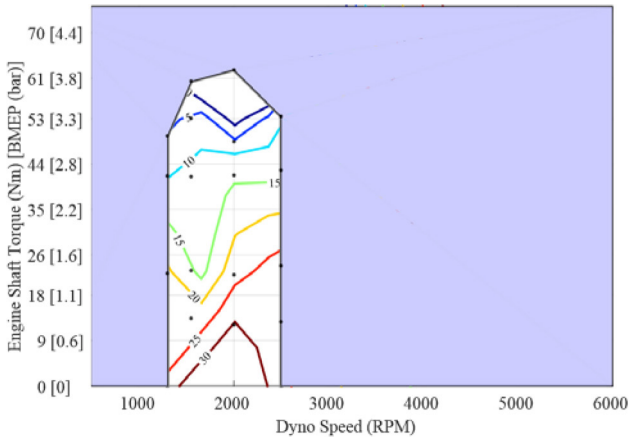


Figure 11. CDA BTE improvement (%) from cEGR four-cylinder operation

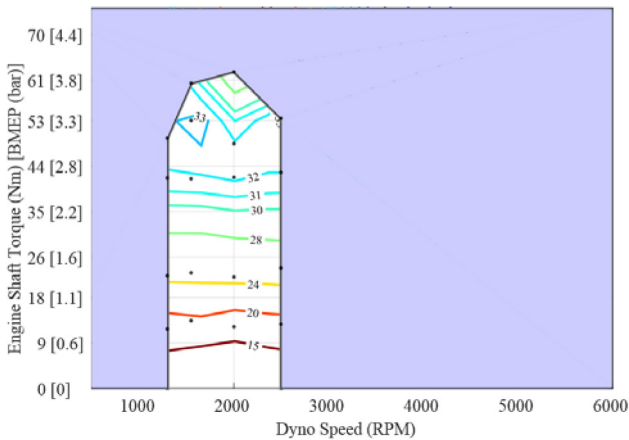


Figure 12. CDA BTE (%)

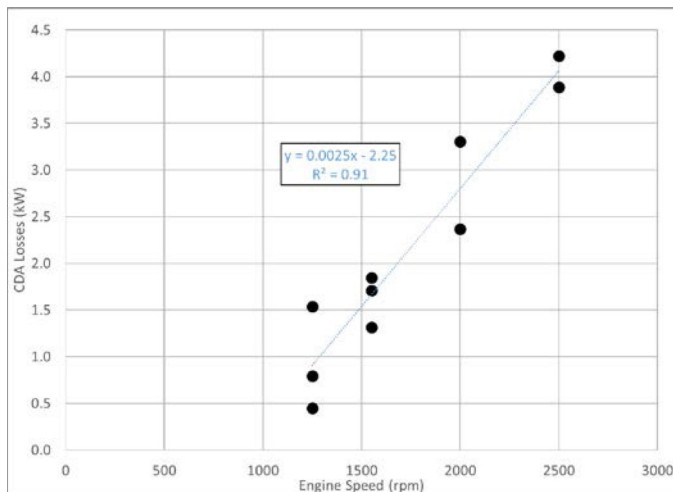


Figure 13. Estimated CDA losses (kW)

Two-Cycle Predictions

Two-cycle CO₂ (regulatory-weighted FTP/HwFET) predictions were conducted to put the cEGR and CDA BTE improvements into context. The first method was to use fuel-weighted steady state modes to predict possible improvements. This method found the eight steady state modes that had the most influence on two-cycle CO₂ emissions. The second method used the measured cEGR and CDA fuel maps as inputs for the ALPHA model to predict results with a future vehicle configuration.

Derivation of 8 Modes

A 2014 Mazda3 with a 6 speed automatic transmission was chassis tested over the two-cycle FTP and HwFET while logging injector duration, fuel rail pressure, and MAF. These parameters were correlated to engine test cell measurements to estimate fuel flow and load (torque). The fuel mass was binned by engine speed and load (Figure 14, top). An algorithm was developed to step through the speed/load bins and determine the bin that was most influential. Influence was calculated as the sum of fuel within a radius from a bin, discounted by distance from the central bin. When a bin was found to be most influential, the fuel bins within its radius were reduced by the amount included in its influence sum (i.e. the distance discounted value). Then the process was repeated to find the next most influential bin. This algorithm was used to determine the 8 modes that captured where most of the fuel was burned over the 2-cycle tests (Figure 14, bottom). Table 3 lists the modes and the fraction of the two-cycle fuel represented by each mode. These modes cover 57% of the total two-cycle fuel consumption.

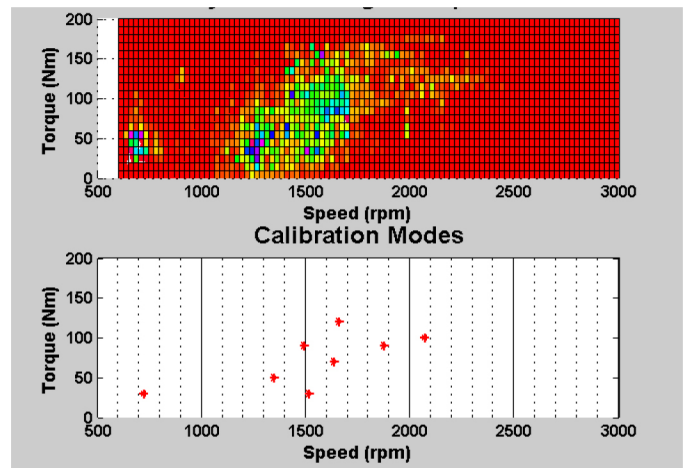


Figure 14. Two-cycle fuel consumption and calibration modes for a 2014 Mazda3 automatic. Dark blue is the most fuel consumed and red is the least fuel consumed (top plot).

8 Mode Results

Since there were many assumptions in this method, only the change in BTE between the 8 modes run with the OEM ECU and cEGR/CDA was calculated as an indication of the improvement that might be seen (Table 3). The cEGR and CDA + cEGR Improvement columns were calculated as BTE improvement from Equation 3. The fuel weighted composite BTE reduction was calculated as shown in Equation (4). The estimated fuel weighted BTE improvement was approximately 6% across the 8 modes with the addition of cEGR.

$$f_{wc} = \frac{\sum imp_k * ffrac_k}{\sum ffrac_k} \quad (4)$$

Where:

f_{wc} is the fuel weighted composite improvement (%)

k is the mode number

imp is the % cEGR Improvement at mode k from [Table 3](#)

$ffrac$ is the % cycle fuel over the two-cycle test represented by mode k from [Table 3](#)

Two of the 8 modes were in the tested CDA range ([Table 3](#)). Modes 2 and 4 were replaced with CDA + cEGR BTE Improvement data and the fuel weighted BTE benefit was recalculated. The resulting fuel weighted composite improvement was approximately 8%.

Table 3. 8 mode two-cycle weighting factors, BTE, and BTE improvements over the baseline 14:1 engine without cEGR.

Mode	Speed (rpm)	Torque (Nm)	Cycle Fuel (%)	cEGR BTE (%)	cEGR Improvement (%)	CDA + cEGR Improvement (%)
1	720	30	9	22.3	13.4	
2	1340	50	9	31.6	4.9	11.2
3	1450	90	6	37.1	4.1	
4	1550	30	4	25.5	8.2	21.0
5	1630	70	14	34.9	3.6	
6	1660	120	4	37.4	6.3	
7	1870	90	6	36.6	3.3	
8	2060	100	5	37.2	9.0	
Fuel weighted composite improvement:					6.4%	8.2%

ALPHA Future Vehicle CO₂ Prediction

The fuel flow data collected in this testing was imported into ALPHA to examine the effect of adding cEGR and CDA on vehicle CO₂ emission rates.

The vehicle chosen for simulation was selected from the future fleet used for the MTE. The transmission was an 8 speed automatic and featured start stop functionality. The vehicle road load coefficients and test weight were derived from the EPA test car database for the 2015 fleet [18]. The exemplar vehicle for the medium power to weight / low road load (MPW_LRL) group was futured by applying 10% mass reduction, 20% aerodynamic drag reduction and 20% rolling resistance improvements yielding the vehicle summarized in [Table 4](#). The results from this set of simulations were presented in [Table 5](#). The FTP cold start correction, an 11% increase in fuel consumption during the first phase as was used for future engines in the MTE, was applied to each simulation.

Table 4. ALPHA vehicle description.

	Future MPW_LRL
ETW	3293
A (lb)	22.12
B (lb/mph)	0.0754
C (lb/mph ²)	0.01594
Final Drive	3.45
Gears	8
Ratios	5.5
	3.473
	2.2
	1.74
	1.33
	1
	0.82
	0.632

Table 5. Simulated two-cycle CO₂ rate in a midsize car featuring additional drivetrain improvements

Engine	FTP CO ₂ g/mi	HWFET CO ₂ g/mi	Combined CO ₂ g/mi	Improvement
OEM cal 14:1 CR	247.0	160.7	208.1	-
14:1 CR + cEGR	222.2	149.8	189.7	7.6%
14:1 CR + cEGR + CDA	217.5	147.2	185.8	9.5%

The overall improvements for both cases are greater than the 8 mode calculation. This difference is likely caused by the slight shift in operation from the addition of the 8 speed transmission in the future car which allowed more high BTE engine operation. The predicted 2 % improvement from adding CDA to cEGR was consistent with the modal estimate for a current vehicle.

Summary/Conclusions

cEGR and CDA were tested on an Atkinson capable engine to determine their impact on CO₂ emissions. BTE maps were generated to study where the technologies were most beneficial. Two-cycle CO₂ emission reduction predictions were made based on a representative set of 8 steady state modes and from ALPHA. Key findings:

1. cEGR moved the peak efficiency further into the two-cycle operating area resulting in a modal projected 6% improvement in two-cycle CO₂ for a current vehicle.
2. The 10-90% combustion durations with cEGR were much longer than optimum. Additional in-cylinder motion would be required to shorten combustion and potentially improve cEGR knock and CO₂ reduction effectiveness.
3. CDA was projected to reduce two-cycle CO₂ emissions by an additional 2% over the current vehicle cEGR case using the 8 mode prediction.

4. CDA lost 3-7% BTE relative to equivalently loaded four-cylinder operation due to the deactivated cylinders. CDA operation was simulated by removing the rockers from cylinders 2 and 3. The permanently deactivated cylinders did not fully represent a production viable system. Consequently, the results should be considered a rough estimate of CDA effectiveness.
5. The cEGR two-cycle CO₂ improvement predicted by ALPHA with a future vehicle was 7.6%.
6. The cEGR and CDA two-cycle CO₂ improvement predicted by ALPHA with a future vehicle was 9.5%.
12. Matsui, J., Koyama, H., Goto, Y., and Kawai, H., "Development of 3.5L V6 Gasoline Direct Injection Engine - ESTEC 2GR-FKS/FXS -," SAE Technical Paper [2015-01-1972](#), 2015, doi:[10.4271/2015-01-1972](#).
13. Mazda Motor Corporation, "MAZDA'S INNOVATIVE SKYACTIV TECHNOLOGIES MAKE U.S. DEBUT", April 21, 2011, http://www.mazdausamedia.com/index.php?s=31676&item=967#assets_67:125272, accessed Sep 2015.
14. Hwang, K., Hwang, I., Lee, H., Park, H. et al., "Development of New High-Efficiency Kappa 1.6L GDI Engine," SAE Technical Paper [2016-01-0667](#), 2016, doi:[10.4271/2016-01-0667](#).
15. Yamada, T., Takahashi, M., Ikeya, K., Takegata, N., "Intake Design for Reduction of Duration of Combustion," Honda R&D Technical Review, Vol. 27, No. 2, p. 71-79, <https://www.hondarandd.jp/>.
16. Ellies, B., Schenk, C., and Dekraker, P., "Benchmarking and Hardware-in-the-Loop Operation of a 2014 MAZDA SkyActiv 2.0L 13:1 Compression Ratio Engine," SAE Technical Paper [2016-01-1007](#), 2016, doi:[10.4271/2016-01-1007](#).
17. Alger, T., Gingrich, J., Roberts, C., Mangold, B. et al., "A High-Energy Continuous Discharge Ignition System for Dilute Engine Applications," SAE Technical Paper [2013-01-1628](#), 2013, doi:[10.4271/2013-01-1628](#).
18. U.S. EPA, "Final Determination on the Appropriateness of the Model Year 2022-2025 Light-Duty Vehicle Greenhouse Gas Emissions Standards under the Midterm Evaluation: Technical Support Document," January, 2017.

References

1. U.S. Environmental Protection Agency and Department of Transportation, "2017 and Later Model Year Light-duty Vehicle Greenhouse Gas Emissions and Corporate Average Fuel Economy Standards: Final Rule," Federal Register vol. 77, no 199, October 15, 2012.
2. Lee, S., Schenk, C., and McDonald, J., "Air Flow Optimization and Calibration in High-Compression-Ratio Naturally Aspirated SI Engines with Cooled-EGR," SAE Technical Paper [2016-01-0565](#), 2016, doi:[10.4271/2016-01-0565](#).
3. Lewis, A., Akehurst, S., Turner, J., Patel, R. et al., "Observations on the Measurement and Performance Impact of Catalyzed vs. Non Catalyzed EGR on a Heavily Downsized DISI Engine," *SAE Int. J. Engines* 7(1):458-467, 2014, doi:[10.4271/2014-01-1196](#).
4. Alger, T., Chauvet, T., and Dimitrova, Z., "Synergies between High EGR Operation and GDI Systems," *SAE Int. J. Engines* 1(1):101-114, 2009, doi:[10.4271/2008-01-0134](#).
5. Kumano, K. and Yamaoka, S., "Analysis of Knocking Suppression Effect of Cooled EGR in Turbo-Charged Gasoline Engine," SAE Technical Paper [2014-01-1217](#), 2014, doi:[10.4271/2014-01-1217](#).
6. Leone, T. and Pozar, M., "Fuel Economy Benefit of Cylinder Deactivation - Sensitivity to Vehicle Application and Operating Constraints," SAE Technical Paper [2001-01-3591](#), 2001, doi:[10.4271/2001-01-3591](#).
7. Falkowski, A., McElwee, M., and Bonne, M., "Design and Development of the DaimlerChrysler 5.7L HEMI® Engine Multi-Displacement Cylinder Deactivation System," SAE Technical Paper [2004-01-2106](#), 2004, doi:[10.4271/2004-01-2106](#).
8. Eichler, F., Demmelbauer-Ebner, W., et al, "The New EA211 TSI® evo from Volkswagen", Vienna International Motorsymposium, 2016.
9. Luria, D., Taitel, Y., and Stotter, A., "The Otto-Atkinson Engine - A New Concept in Automotive Economy," SAE Technical Paper [820352](#), 1982, doi:[10.4271/820352](#).
10. Wan, Y. and Du, A., "Reducing Part Load Pumping Loss and Improving Thermal Efficiency through High Compression Ratio Over-Expanded Cycle," SAE Technical Paper [2013-01-1744](#), 2013, doi:[10.4271/2013-01-1744](#).
11. Wang, C., Daniel, R., and Xu, H., "Research of the Atkinson Cycle in the Spark Ignition Engine," SAE Technical Paper [2012-01-0390](#), 2012, doi:[10.4271/2012-01-0390](#).

Contact Information

The author can be reached at

schenk.charles@epa.gov

Acknowledgments

The author would like to acknowledge the efforts of SwRI and Pi Innovo which were instrumental to the success of this project. The role of these organizations did not include establishing Agency policy. This testing was made possible by the continuing support of the EPA NCAT team.

Definitions/Abbreviations

AKI - Anti-knock index, (RON+MON)/2

ALPHA - Advanced Light-Duty Powertrain and Hybrid Analysis

ATDC - After top dead center

BMEP - Brake mean effective pressure

BTDC - Before top dead center

BSFC - Brake specific fuel consumption

BTE - Brake thermal efficiency

CA50 - 50% burn location (CAD ATDC)

CAD - Crankshaft angle degrees (°)

CAFE - Corporate Average Fuel Economy

CDA - Cylinder deactivation

cEGR - Cooled external exhaust gas recirculation

COV - IMEP coefficient of variation

ECU - Engine control unit

EPA - Environmental Protection Agency

ETW - Equivalent test weight, roughly curb weight (dry) + 300 lbs

FTP - Federal test procedure FTP-75; in this paper, a 3-bag LA4

GDI - Gasoline direct injection

GHG - Greenhouse gas

HIL - Hardware-in-the-loop

HWFET - Highway fuel economy test procedure

iEGR - Internal exhaust gas recirculation

IMEP - Indicated mean effective pressure

IVC - Intake valve close

LD - Light duty

LIVC - Late intake valve close

MTE - Midterm Evaluation

NHTSA - National Highway Traffic Safety Administration

NVH - Noise, vibration, and harshness

OEM - Original equipment manufacturer; production parts

RRC - Rolling resistance coefficient

TAR - Technical Assessment Report

TDC - Top dead center firing

VSIM - Virtual simulation

The Engineering Meetings Board has approved this paper for publication. It has successfully completed SAE's peer review process under the supervision of the session organizer. This process requires a minimum of three (3) reviews by industry experts.

This is a work of a Government and is not subject to copyright protection. Foreign copyrights may apply. The Government under which this paper was written assumes no liability or responsibility for the contents of this paper or the use of this paper, nor is it endorsing any manufacturers, products, or services cited herein and any trade name that may appear in the paper has been included only because it is essential to the contents of the paper.

Positions and opinions advanced in this paper are those of the author(s) and not necessarily those of SAE International. The author is solely responsible for the content of the paper.

ISSN 0148-7191

<http://papers.sae.org/2017-01-1016>